aerospace

MDPI

Review

A Review of the Current Status of Active Cooling Technology of Liquid Metal for Hypersonic Aircraft

Haowei Li *, Zhongwei Deng, Xuran Hou and Guangze Song

College of Ocean Engineering and Energy, Guangdong Ocean University, No. 1, Haida Road, Zhanjiang 524088, China; 18300137687@stu.gdou.edu.cn (Z.D.); houxuran@stu.gdou.edu.cn (X.H.); sgz@stu.gdou.edu.cn (G.S.)

* Correspondence: lhw_hit@163.com

Abstract

Under high-Mach-number flight conditions, the combustion chambers of hypersonic vehicles encounter extreme thermal environments marked by unilateral heating, high-heat-flux density, and supercritical pressure. Traditional hydrocarbon fuel cooling often suffers from insufficient heat sinks, high-temperature cracking and coking blockages, making it difficult to meet long-endurance thermal protection requirements. Liquid metal, due to its extremely high thermal conductivity, wide liquid phase temperature range, low Prandtl number and electromagnetic pump driving capability, has become a key technology for breaking through the bottleneck of high-heat-flux thermal protection. Apart from the magnitude of heat flux, the heat-transfer time scale (such as the characteristic thermal response time of the wall and the fluid) is also crucial. During hypersonic flight, transient thermal loads can change within milliseconds, requiring rapid thermal response. Liquid metals, due to their high thermal diffusivity, have a shorter thermal diffusion time compared to hydrocarbon fuels. This review employs a systematic literature review of approaches using gallium-indium-tin alloy, GaInSn, focusing on three core directions: the flow and heat-transfer characteristics of liquid metals, the optimization of cooling micro-channels, and the application of thermal protection systems. It summarizes the research progress at home and abroad, compares and analyzes the performance differences and applicable scenarios of typical liquid-metal working fluids, and summarizes the advantages and disadvantages of existing models, structural designs, and system schemes. The research shows that liquid metals can significantly alleviate thermal stratification and eliminate coking, and deep, narrow, tree-shaped, and biomimetic micro-channels can effectively enhance heat transfer. The liquid-metal-fuel dual-channel waste heat recovery and thermoelectric power generation system has demonstrated engineering application potential. Currently, the field still faces key challenges, such as unclear heat-transfer mechanisms under extreme conditions, the lack of general heat-transfer correlation formulas, insufficient compatibility with high-temperature materials, poor miniaturization and vibration resistance of electromagnetic pumps, and low system integration. In the future, efforts should be focused on developing multi-field coupled heat-transfer models under extreme thermal environments using engineered micro-channel structures, corrosion-resistant materials, and lightweight electromagnetic pumps, promoting the research and development of integrated thermal protection, heating and power generation systems, and providing support for the development of advanced thermal management systems for hypersonic aircraft and aviation engines.

Keywords: hypersonic aircraft; liquid-metal cooling; active thermal protection; flow and heat transfer; thermal management

Check for updates

Academic Editor: Xiande Fang

Received: 3 July 2026
Revised: 31 July 2026
Accepted: 12 August 2026
Published: 14 August 2026

Copyright: © 2026 by the authors. Licensee MDPI, Basel, Switzerland. This article is an open access article distributed under the terms and conditions of the Creative Commons Attribution (CC BY) license.

1. Research Background

In recent years, hypersonic vehicles, as a new generation of aircraft, have attracted extensive research worldwide [1–3]. Hyper-ramjet engines are considered one of the most promising propulsion systems for high-Mach-number hypersonic vehicles [4–6]. However, the thermal protection system for scramjet engines at high Mach numbers is of critical importance for the further development of these engines. As the Mach number increases, the wall heat load gradually exceeds the upper limit of the fuel's heat absorption capacity, making insufficient fuel heat sinks the core limitation of wall-cooling technology [7]. Coking issues arising from fuel pyrolysis at high temperatures can easily clog wall-cooling channels, causing wall-cooling failure and potentially leading to complete destruction of the combustion chamber walls [8]. Table 1 provides a detailed breakdown of the extreme conditions of the cooling channels in hypersonic aircraft. Liquid-metal cooling is a highly efficient [9], high-throughput heat dissipation method with an extremely broad range of applications. Liquid metals, owing to their superior thermal properties and neutron characteristics, can dissipate more heat than water coolants of equivalent mass flow rate, making them highly promising reactor coolants. In recent years, liquid metals have attracted significant attention as circulating working fluids due to their extremely high thermal conductivity and relatively low Prandtl number [10]. Among them, sodium (Na) achieves a thermal conductivity of 80–90 W/m·K, with a Prandtl number of approximately 0.005 in the 400–800 °C range, providing excellent transient response capability; gallium-based alloys remain liquid over a wide temperature range. Through simulation studies of heat transfer in rectangular channels on combustion chamber walls, it was found that the convective heat-transfer coefficient of GaInSn is significantly higher than that of n-decane, and it can effectively reduce thermal stratification within hydrocarbon fuel channels. Cheng et al. [11] compared the wall-cooling performance of supercharged ramjet engines using hydrogen and liquid sodium. The study found that under identical heater hot-side inlet temperatures and fuel equivalence ratios, liquid sodium cooling reduced the peak wall temperature of the combustion chamber by up to 6.15%. These advantages stem not only from high-heat-flux handling capacity but also from millisecond-scale transient thermal response times.

Table 1. The extreme conditions of the cooling channels of hypersonic aircraft.

Environmental Characteristics	Physical Performance	Engineering Challenge
Heat load	Unilateral heating, heat flux density > 1 MW/m^2	The wall surface temperature is extremely uneven, with concentrated thermal stress, which makes it prone to thermal fatigue failure.
Fluid state	The wall surface temperature is extremely uneven, with concentrated thermal stress, which makes it prone to thermal fatigue failure.	Significant changes in physical properties (such as density and specific heat) occur, leading to "pseudo-phase transition", and traditional heat-transfer formulas become invalid.
Chemical properties	High-temperature pyrolysis (T > 600 °C)	Fuel carbonization blocks the channels; endothermic reactions occur simultaneously with increased flow resistance.
Mechanical environment	Thermal-fluid–solid strong coupling	Channel deformation leads to changes in flow resistance; vibration and pulsating thermal loads cause structural damage.

Hydrocarbon fuels used in regenerative cooling channels may undergo thermal cracking reactions under high-temperature conditions. When the fuel temperature exceeds the critical threshold, fuel molecules decompose and generate coke precursors. These precursors accumulate near the wall under the influence of temperature and concentration gradients, eventually forming solid carbon deposits, which can increase flow resistance and deteriorate cooling performance. When the temperature of supercritical hydrocarbon fuels exceeds the critical threshold of 400 °C, fuel molecules undergo cracking reactions due to thermodynamic instability. A large number of coking precursors locally accumulate in near-

wall regions under the influence of temperature and concentration gradients, forming solid carbon deposits. Current research indicates that aromatic hydrocarbons are most prone to causing coking [12]. The thermal conductivity of liquid metal is significantly higher than that of traditional hydrocarbon fuels, offering superior heat-transfer capabilities that enable rapid heat dissipation. Therefore, when liquid metal is used as the cooling working fluid in hypersonic ramjet engines, adjusting the liquid-metal flow rate can induce an "isothermal" distribution of combustion chamber wall temperatures. This reduces the heat-transfer density from the combustion gases to the walls, thereby decreasing the cooling load on the working fluid [13]. To provide an intuitive understanding of the differences between the two, Table 2 compares the primary physical properties of typical liquid metals $Ga_{68}In_{20}Sn_{12}$ and sodium (Na) with those of the representative hydrocarbon fuel, toluene. Toluene stands out among traditional hydrocarbon fuels due to its low-temperature adaptability at −95 °C and its specific heat capacity of 1700 $J \cdot kg^{-1} \cdot K^{-1}$. However, its low boiling point of 110.6 °C causes rapid vaporization and pyrolysis coking under superheated combustion conditions, leading to deteriorated phase-change heat transfer.

Table 2. Comparison of thermophysical properties of toluene, GaInSn, and sodium.

Working Fluid	Melting Point/°C	Boiling Point/°C	Density/($kg \cdot m^{-3}$)	Specific Heat/($J \cdot kg^{-1} \cdot K^{-1}$)	Thermal Conductivity/($W \cdot m^{-1} \cdot K^{-1}$)	Viscosity/(10^{-3} Pa·s)	Electrical Conductivity/(10^6 $S \cdot m^{-1}$)
Toluene (representative hydrocarbon fuel)	−95	110.6	867	1700	0.133	~1	Negligible
$Ga_{68}In_{20}Sn_{12}$	10.7	2200	6363	366	39	~2	6.8
Sodium (Na)	97.8	883	~930	~1300	80–90	~0.3	20–30

In contrast, liquid metals demonstrate significant superiority. $Ga_{68}In_{20}Sn_{12}$ has a low melting point of 10.7 °C and a high boiling point of approximately 2200 °C, maintaining a single liquid phase across an ultra-wide temperature range of −10.7~2200 °C, fundamentally avoiding phase-change heat-transfer degradation. Sodium (Na), on the other hand, exhibits extremely high thermal conductivity (80–90 $W \cdot m^{-1} \cdot K^{-1}$) and a very low Prandtl number (≈0.005) in the 400–800 °C range, providing excellent millisecond-scale transient thermal response capability.

In terms of heat-transfer efficiency, the thermal conductivity of liquid metals (39 $W \cdot m^{-1} \cdot K^{-1}$ for $Ga_{68}In_{20}Sn_{12}$ and 80–90 $W \cdot m^{-1} \cdot K^{-1}$ for Na) is two orders of magnitude higher than that of toluene at 0.133 $W \cdot m^{-1} \cdot K^{-1}$. Combined with a high density (6363 $kg \cdot m^{-3}$ for $Ga_{68}In_{20}Sn_{12}$), this yields a volumetric heat capacity of approximately 2.33 $MJ \cdot m^{-3} \cdot K^{-1}$, thereby achieving the dual objectives of rapid heat conduction and large heat sink storage. These advantages arise not only from high-heat-flux capacity but also from shorter thermal diffusion time scales compared with hydrocarbon fuels. Although the viscosity of liquid metals at ~2.0×10^{-3} Pa·s is slightly higher than that of toluene, their ultra-high electrical conductivity (6.8×10^6 $S \cdot m^{-1}$ for $Ga_{68}In_{20}Sn_{12}$ and even higher for Na) enables electromagnetic pump-driven circulation schemes, eliminating moving parts and thereby enhancing system efficiency and stability.

Thermal management has always been a key bottleneck restricting the development of hypersonic aircraft. Liquid metals, due to their excellent heat dissipation capabilities, have become a research hotspot in the field of thermal management for hypersonic aircraft. Domestic and international researchers have conducted extensive and in-depth studies on the application of liquid metals in hypersonic thermal management, and the system configurations have become increasingly diverse. In addition to the Rankine cycle and closed Brayton system based on liquid metals, innovative integration of liquid metals with hydrocarbon fuels has also been explored, including dual-channel cooling cycles and thermoelectric conversion schemes for combined thermal protection and power generation.

These methods have been proven to provide wall cooling and residual heat recovery effects superior to traditional regenerative cooling while alleviating challenges such as coking and insufficient heat sinks.

2. Current Status of Liquid-Metal Cooling Performance in Hypersonic Vehicles

Thermal management has consistently posed a critical bottleneck in the development of both hypersonic vehicles and aero-engines. Liquid metals with high heat dissipation capabilities have gradually emerged as a research hotspot in the field of hypersonic vehicle thermal management. Scholars both domestically and internationally have conducted extensive and in-depth research on the application of liquid metals in hypersonic vehicles, with related application forms becoming increasingly diverse.

Under Mach 6–8 flight conditions with heat flux densities of 1–5 MW/m^2 (and millisecond-scale heat-transfer times due to high-velocity flows), previous studies have quantified effective wall-cooling performance (Xu et al. [14] for aero-engine comparisons at high heat fluxes). In particular, extreme heat flux conditions (often exceeding 1–5 MW/m^2) in scramjet combustion chambers have been addressed through liquid-metal applications, demonstrating significant reductions in wall temperature peaks and thermal stratification.

In addition to liquid-metal-based Rankine cycles and closed-loop Brayton systems, Cheng et al. [13] presents a comprehensive study on energy management systems for scramjet engines under limited cold source conditions, proposing a power generation scheme based on a basic reheat-type and recompression-type supercritical carbon dioxide closed Brayton cycle (sCO_2-CBC). Liquid sodium serves as the intermediate heat-transfer medium, absorbing thermal energy from the engine cooling passages and transferring it to the Brayton cycle via a heat exchanger. Hydrogen functions as the cycle's cooling source. Research indicates that using liquid sodium with a high heat-transfer coefficient as the direct heating medium in closed-loop power generation systems for hypersonic vehicles can achieve superior wall thermal protection and thermoelectric conversion performance. Compared to hydrocarbon fuels in regenerative cooling systems, liquid metal exhibits no coking within high-temperature passages, effectively protecting combustion chamber walls. Recent complementary studies have further advanced the field: Su et al. [15] investigated the molecular dynamics of liquid sodium boiling characteristics under different wall temperatures, providing insights into incipient boiling superheat, heat-transfer performance, and underlying mechanisms; Yao et al. [16] reviewed the thermophysical properties of liquid gallium; Xu et al. [14] compared heat-transfer performance between liquid metal and aviation kerosene in aero-engine wall-cooling channels; and Wang et al. [17] explored liquid-metal microchannel cooling for aerospace thermal management. Liquid sodium properties (melting point ~98 °C, boiling point ~883 °C, thermal conductivity ~80–90 W/(m·K) at operating temperatures) complement those of gallium-based alloys such as $Ga_{68}In_{20}Sn_{12}$ and support broader applications across hypersonic and aero-engine contexts.

Traditional regenerative cooling systems mainly rely on hydrocarbon fuel as the cooling medium. The fuel absorbs heat from the combustion chamber wall through cooling channels and then enters the combustion process, realizing both thermal protection and fuel utilization. However, the cooling capability is limited by the heat sink capacity and high-temperature cracking characteristics of hydrocarbon fuels.

Compared with fuel-based cooling, liquid-metal cooling introduces an independent high-performance heat-transfer medium. Liquid metal absorbs heat from the cooling channels and transfers it through heat exchangers or power-generation systems, avoiding fuel pyrolysis and improving high-temperature thermal management capability [13].

Xu et al. [18] proposes a novel thermal management scheme for scramjet engines based on the alkali metal Rankine cycle. During extended flights, this system achieves a 32.22%

fuel savings rate, significantly enhancing the aircraft's overall performance by substantially reducing the weight penalty associated with carrying excess fuel. The power output of the power generation system reaches 32.22% of its cycle capacity. Through system parameter optimization and component efficiency enhancements, the cycle efficiency is expected to improve further.

With advances in semiconductor materials, domestic scholars have introduced semiconductor materials into the field of direct thermoelectric conversion. Cheng et al. [19] proposes a cooling and power generation scheme for hypersonic vehicles based on semiconductor materials. A liquid-metal-based thermoelectric conversion system integrates thermal protection and waste heat recovery. In this configuration, liquid metal serves as both a circulating coolant and a heat-transfer medium, transferring the absorbed thermal energy to thermoelectric modules for direct power generation. The system provides an alternative approach for improving the overall energy utilization efficiency of hypersonic vehicles [19]. Through comparative analysis, it was found that three to four thermoelectric stages yield the optimal power generation efficiency. Additionally, the study introduces the concept of using liquid metal as a circulating heat source and wall-cooling medium, comparing it with fuel-based thermal energy supply modules utilizing regenerative cooling. Results indicate that the liquid-metal-based approach delivers superior combined heat and power supply capabilities while ensuring effective thermal protection for wall surfaces.

Xu et al. [20] proposed a dual-layer cooling channel configuration combining liquid metal and hydrocarbon fuel. In this structure, liquid metal provides high-efficiency heat transfer near the high-temperature wall, while hydrocarbon fuel participates in heat absorption and energy utilization. The dual-channel design reduces temperature non-uniformity and improves cooling stability under high-heat-flux conditions [20]. Research indicates that under extreme operating conditions, compared to single-channel n-decane cooling, the dual-channel n-decane side significantly reduces the peak temperature field non-uniformity from approximately 55% in the single-channel configuration to below 18%. Furthermore, the maximum non-uniformity coefficient for cracking rates is substantially lowered from 1000% in the single-channel setup to less than 100% in the dual-channel configuration. Compared to single-channel liquid-metal cooling, the dual-channel liquid-metal side reduces the maximum heat sink unevenness coefficient from 230% in single-channel systems to approximately 80%. The dual-channel liquid metal-hydrocarbon fuel structure design not only significantly enhances high-temperature waste-heat recovery efficiency but also provides more stable cooling assurance for high-heat-flux density scenarios.

Based on these applications, the flow and heat-transfer characteristics of liquid metals are crucial for further optimizing thermal management systems.

3. Liquid-Metal Flow and Heat-Transfer Characteristics

The flow and heat-transfer characteristics of liquid metals are influenced by multiple coupled factors. This section systematically reviews the research progress from three dimensions: the influence of fluid properties, geometric parameters, and flow conditions. Firstly, it summarizes the heat-transfer correlations applicable to different working conditions; secondly, it analyzes the influence laws of factors such as pipe cross-sectional shape, inclination angle (buoyancy force), inlet flow velocity, and wall roughness on heat transfer; finally, it explores the optimization design of micro-channel structures and its enhancement effect on heat-transfer performance.

Xiang et al. [21] conducted a numerical simulation and factor analysis study of the natural circulation heat-transfer characteristics of four typical liquid metals (sodium, sodium-potassium alloy, lead, and lead-bismuth alloy) using CFX software. The performance of different metals under extreme heat flux conditions shows significant differences.

Liquid sodium exhibits a unique negative correlation. As the heating power increases, its heat-transfer coefficient actually decreases. This is because the thermal conductivity of sodium decreases significantly with an increase in temperature, and this inhibitory effect outweighs the promoting effect brought about by the increase in temperature difference.

Lead and lead-bismuth alloys show a positive correlation. As the power increases, the heat-transfer coefficient also increases. This is because the thermal conductivity of lead-based materials is less affected by temperature, and the enhanced thermal drive caused by the increase in temperature difference becomes the dominant factor.

The sodium-potassium alloy shows a nonlinear characteristic (first rises then drops). In the low-power region, the thermal conductivity and temperature difference jointly promote heat transfer; but in the high-power region, the inhibitory effect of the decrease in thermal conductivity exceeds the promoting effect of the temperature difference, resulting in a decrease in the coefficient.

Developing appropriate heat-transfer correlation equations for liquid-metal flow characteristics under different operating conditions is crucial for understanding the related thermal properties and enabling engineering applications. Building upon existing correlation equations for specific operating conditions, this study analyzes the effects of cooling-pipe cross-sectional geometry and inlet velocity on the flow and heat transfer of liquid metal within the pipes.

3.1. Heat Exchange Correlation

In the high-heat-flux environment of a scramjet combustion chamber, liquid metals exhibit high thermal conductivity, extremely low Prandtl number, and excellent flow stability compared with aviation kerosene. Their heat-transfer mechanisms differ significantly from those of conventional fluids, necessitating new theoretical models for practical engineering applications [22]. Since the mid-20th century, systematic studies have been conducted on liquid-metal heat transfer; however, no universal correlation exists that covers the extreme conditions (heat flux 1–5 MW/m^2, unilateral heating, Mach 5–8 or aero-engine-relevant lower-Mach sustained flight) encountered in hypersonic vehicles.

Most existing correlations were developed or extrapolated under specific conditions—circular tubes, annular ducts, rod bundles, or moderate heat fluxes (typically <1 MW/m^2 for sodium/lead-bismuth, lower for gallium alloys)—often using mercury or sodium as working fluids. These correlations are commonly extrapolated to hypersonic applications, but their accuracy under high heat flux, variable properties, and buoyancy effects remains limited. The main correlations and their conditions are summarized below.

Martinelli [23] first established a theoretical framework for liquid-metal heat transfer by applying the analogy between turbulent momentum and energy transport while accounting for molecular conduction. This served as the foundation for subsequent models but lacks corrections for extreme property variations.

Lyon [24] and Dwyer [25] derived heat-transfer equations for turbulent flow in circular tubes, incorporating the turbulent Prandtl number and molecular conduction effects. These are suitable for fully developed flow in circular pipes under moderate heat flux but show large errors (>20–30%) under high heat flux (>1 MW/m^2) and significant property changes.

Maresca and Dwyer [26] extended the model to rod-bundle channels based on mercury experiments, making it applicable to complex core-like geometries but difficult to map directly to simple wall-cooling channels.

Werner et al. [27] and later Shi et al. [28] performed experiments on sodium and sodium-potassium alloys in circular and annular tubes, deriving fitted correlations via least-squares methods. Shi et al. additionally considered eccentricity effects in sleeve tubes within heat flux ranges of 12–59 MW/m^2 (though most data were at lower fluxes).

Wang et al. [29] conducted experiments and 3D simulations on lead-bismuth eutectic in circular tubes, obtaining alloy-specific correlations with average errors around 10% under their test conditions.

Xu et al. [30] highlighted the challenges in low-Prandtl-number fluid simulations and emphasized the need for new models and advanced instrumentation for hypersonic-relevant conditions.

Table 3 summarizes the applicability and limitations of representative correlations. Under hypersonic conditions, the primary shortcomings are insufficient consideration of high heat flux (>1 MW/m^2) and strong multi-physics coupling. Overall, while existing correlations provide valuable references, they cannot meet the requirements of hypersonic vehicles (Mach 5–8, heat flux 1–5 MW/m^2).

Table 3. Comparison of different linkage forms.

Correlation/Source of Research	Applicable Conditions	Advantages	Disadvantages and Limitations	Error/Note
Martinelli Theory [24]	Theoretical basis for heat transfer in liquid metals	A theoretical framework for heat transfer in liquid metals was established, and the turbulent dynamics were compared with energy transfer.	Based on theoretical derivation, it lacks corrections for extreme working conditions.	The document states that it serves as the foundation for subsequent research.
Lyon/Dwyer [25,26]	Turbulent heat transfer in a circular pipe	Taking into account the molecular heat conduction effect, it can better predict the basic heat-transfer law within the circular tube.	Without taking into account the significant changes in physical properties, the prediction error is large.	The error is significant under high heat flow and needs to be corrected
Maresca and Dwyer [27,28]	Rod bundle channel	Suitable for simulating complex core structures; takes into account the flow of fluids in the densely arranged structure.	The structure is complex and difficult to directly map into the simple design of a wall-cooling channel.	Based on mercury experimental data
Werner and Cotta [28]	Based on the least squares method for fitting	Special calibration was carried out for liquid metal containing heavy metals.	Limited to specific NaK alloy conditions; applicability to high-heat-flux hypersonic channels is uncertain.	The average error is approximately 10% (under specific conditions)
Shi Shuangkai et al. (sodium alloy) [30]	Liquid sodium in circular and annular/sleeve tubes	The influence of the eccentricity factor on the heat-transfer coefficient and the circumferential temperature distribution was considered.	The experimental heat flux range is limited, and it may fail for hypersonic conditions with higher heat fluxes.	Based on the least squares method for fitting

According to the current research, there is no unified and applicable flow and heat-transfer model and general correlation equation for liquid metals under the extreme conditions of hypersonic aircraft. The reasons for this are diverse and can be summarized as follows, as shown in Table 4.

Table 4. Main reasons for the lack of a unified flow and heat-transfer model for liquid metals.

Category	The Main Reason
Thermal properties of the working medium	The thermal properties of sodium-based, lead-based and gallium-based alloys vary significantly, and the heat exchange behavior and laws are difficult to describe in a uniform and unified format.
Extreme condition coupling	Liquid-metal cooling channels in aero-engine or hypersonic applications may operate under highly coupled extreme conditions, including one-sided or non-uniform heating, ultra-high heat flux, high operating pressure, variable gravity or acceleration fields induced by flight attitude changes, and strong thermal fluid–structural coupling. These factors can significantly modify the velocity field, temperature field, boundary-layer development, and wall heat-transfer characteristics. Therefore, simplified assumptions commonly used in conventional forced-convection correlations may not be adequate under such conditions.

Table 4. *Cont.*

Category	The Main Reason
The flow channel structure is diverse	The flow channel shapes such as circular pipes, micro rectangles, tree shapes, T-Y types, and biomimetic vascular types vary greatly, making it difficult to unify the development laws of the flow field and boundary layer.
Fragmentation of experimental data	The working fluids, heat fluxes, flow velocities, and flow channel structures used in each study are not uniform. There are also differences in the experimental platforms and testing methods, making it difficult to cross-verify the data.
The heat-transfer mechanism is still not clear	Liquid metal is a low-Prandtl-number fluid, with molecular conduction being the dominant factor. The turbulent transfer mechanism is quite different from that of conventional fluids, and the relevant theories still need to be further developed.
Engineering factors were not taken into account	Practical constraints such as high-temperature corrosion, material compatibility, and electromagnetic drive have not yet been effectively integrated into the theoretical model.

3.2. Influence of Cooling Pipe Cross-Section Geometry and Inlet Velocity

During forced flow in heated pipes, both vertical and horizontal pipes are subject to buoyancy effects. When fluid flows upward, buoyancy causes heat-transfer deterioration; conversely, when fluid flows downward, buoyancy enhances the heat-transfer process [31]. For low-Prandtl-number liquid metals, buoyancy can modify the mean velocity profile and turbulent heat transport, so its effect should be considered when the channel orientation changes relative to gravity.

Yuan et al. [32] investigated the flow and heat-transfer characteristics of liquid lead-bismuth alloy subjected to buoyancy forces within a horizontal circular pipe. Research has found that under uniform heating conditions around the circumference of a circular tube, a small buoyancy force suppresses the formation of turbulent boundary layer structures in liquid lead-bismuth alloys, thereby weakening turbulence. However, as the buoyancy force increases, turbulence in the liquid lead-bismuth alloy intensifies, leading to enhanced heat-transfer capacity. Dzodzo [33] conducted experiments on turbulent mercury flow within a vertically mounted circular tube to investigate the effect of buoyancy forces on heat-transfer efficiency during liquid-metal flow within the tube. Numerical simulations were conducted on the mixed convection velocity and temperature field of liquid metal in vertical pipes and channels. The Re range was 1000–50,000. Both moderate-buoyancy and high-buoyancy upward/downward flows were considered. The predicted results were compared with the experimental velocity and temperature distributions of the system. Guo et al. [34] conducted experiments on the mixed convective heat transfer of liquid sodium in a vertical circular tube. By applying different heat flux densities to the tube wall to alter the buoyancy force acting on the liquid sodium, it was found that heat transfer was enhanced when buoyancy assisted flow, whereas it was weakened when buoyancy suppressed flow. This occurs because the buoyancy force induces deformation in the velocity distribution of the liquid sodium, thereby altering the convective heat-transfer conditions within the tube. In level flight, the aircraft maintains an approximately constant altitude, and the forced flow in straight cooling channels can usually be approximated as horizontal relative to gravity, depending on the installation direction of the channel. During climb or descent maneuvers, the channel may become inclined relative to gravity, and the flow may therefore have an upward or downward component. The relevant inclination angle is determined by the channel layout and the aircraft attitude or flight-path angle rather than being simply equal to the aerodynamic angle of attack. Under such conditions, buoyancy may assist or oppose the main forced flow, resulting in mixed convection and changes in the local velocity field, temperature field, and heat-transfer coefficient. Guo et al. [35] investigated the variation in buoyancy force by adjusting the angle between the circular tube and the numerical direction. The study revealed that, under fixed inlet and outlet temperatures of the circular tube, liquid metal exhibited distinct heat-transfer characteristics at different angles between the tube and the vertical direction. Vasil'ev et al. [36]

revealed that the Nusselt number strongly depends on the pipe's inclination angle relative to the vertical direction. When the inclination angle is 65° from the vertical, liquid sodium exhibits optimal heat-transfer performance.

Apart from the buoyancy force and the pipe inclination angle, the inlet flow velocity is another crucial flow condition that affects the convective heat transfer of liquid metals. The role of inlet velocity is not limited to turbulence intensity or boundary-layer development. More generally, the magnitude and distribution of velocity determine the Reynolds number, Peclet number, residence time, wall shear stress, and development of hydrodynamic and thermal boundary layers, all of which are directly related to convective heat transfer and pressure loss. For liquid metals with very low Prandtl numbers, heat conduction in the fluid is strong, so the increase in Nusselt number with velocity may be different from that of conventional fluids. Therefore, inlet velocity should be evaluated by considering both heat-transfer enhancement and pumping-power penalty.

Wu et al. [37] obtained a circular cross-section microchannel suitable for liquid metallic lithium through numerical calculations, revealing that the inlet velocity significantly affects both flow and heat-transfer performance. As the inlet velocity increased from 1 m/s to 9 m/s, the pressure drop increased by a factor of 65, while the heat-transfer coefficient improved by approximately 74.35%. Xi et al. [38] investigated the convective heat-transfer characteristics of liquid lead-bismuth alloy in a circular pipe under forced circulation conditions. Research findings indicate that at a fixed wall heat flux density, as the inlet Reynolds number of the liquid lead-bismuth alloy increases, the temperature gradient across the same cross-section along the flow direction gradually decreases while the Nusselt number increases. Therefore, increasing the inlet Reynolds number of the liquid lead-bismuth alloy can significantly enhance its heat-transfer performance. Fico et al. [39] investigated the flow and heat transfer of liquid sodium in a circular channel. The study determined the friction coefficient of liquid sodium under different flow conditions within the pipe. It was also found that during convective heat transfer, the Nusselt number (Nu) slightly increased with a rising power number (Pe), indicating a slight enhancement in convective heat-transfer performance.

Furthermore, artificial roughness on the inner wall of the channel is a commonly used passive heat-transfer enhancement method. Wall roughness can disturb the near-wall velocity and thermal boundary layers, promote vortices or secondary flows, and increase fluid mixing near the heated wall. However, these mechanisms are well established in conventional heat-transfer studies, and their engineering value for liquid-metal cooling should be assessed together with the additional pressure drop, manufacturing feasibility, and possible corrosion or deposition risks. Kadivar and Garg [40] reviewed turbulent heat transfer over rough surfaces. Surface roughness and corrugated channels are widely used passive heat-transfer enhancement strategies because they can disturb the near-wall thermal boundary layer, induce vortices and secondary flows, and increase velocity fluctuations, thereby improving the Nusselt number and temperature uniformity [41,42].

From the perspective of engineering application requirements, existing studies have established some heat-transfer correlations for specific working conditions. However, a universal theoretical model for liquid-metal heat transfer remains unavailable, particularly because the coupled effects of high heat flux, non-uniform heating, channel orientation, variable thermophysical properties, pressure loss, and material compatibility have not been fully clarified. At the macroscopic scale, channel cross-section, inclination angle, inlet velocity, and wall roughness significantly affect the flow and heat-transfer behavior of liquid metals. These factors provide the basis for further geometric optimization. Section 3.3 therefore turns to microchannel structures, where reducing the channel scale

and optimizing the flow-path topology may further enhance heat transfer beyond that achievable in conventional straight channels.

3.3. Microchannel Structure Optimization

3.3.1. Introduction to Microchannels

As discussed in Section 3.2, macroscopic parameters such as channel cross-section, inclination angle, inlet velocity, and wall roughness can significantly affect the flow and heat transfer of liquid metals. However, further heat-transfer enhancement can also be achieved by reducing the characteristic channel scale and optimizing the flow-path topology. Therefore, this section shifts from macroscopic channel parameters to microchannel structure optimization. Microchannels are an effective method for enhancing convective heat transfer. In microchannels, the reduced hydraulic diameter increases the surface-area-to-volume ratio and shortens the heat conduction path from the wall to the bulk fluid. Although the hydrodynamic and thermal boundary layers still develop along the streamwise direction, the small characteristic length makes wall effects more prominent and strengthens the coupling between velocity distribution and temperature distribution. As a result, microchannels can improve heat-transfer performance within a limited cooling volume. Compared to conventional coolants with high-temperature instability and limited convective heat-transfer capabilities, liquid metals possess outstanding thermophysical properties. This material exhibits excellent convective heat-transfer capacity and can operate stably at high temperatures. Currently, high-performance microchannels using liquid metals as coolants are extensively researched [43,44]. The heat-transfer performance of liquid metals in microchannels is strongly influenced by the channel geometry. Key structural parameters include channel height, channel width, fin thickness, fin spacing, inlet/outlet arrangement, branching angle, and flow distribution path. These parameters not only determine the heat-transfer area and thermal resistance but also affect pressure drop, flow maldistribution, and manufacturing feasibility. Therefore, microchannel structural optimization is an important approach for improving liquid-metal cooling performance [45].

Zhao et al. [46] have thoroughly investigated the geometric factors of rectangular straight microchannel heat sinks, including fin height, channel width, and substrate thickness. Zhao [47] analyzed the flow and heat-transfer characteristics of liquid metal in microchannel liquid-cooled cold plates. The research findings indicate that increasing the fluid velocity within the microchannel liquid-cooled cold plate effectively reduces the plate's total thermal resistance but correspondingly increases its pressure drop. Similarly, increasing fin height significantly lowers the total thermal resistance, though it also markedly elevates the pressure drop. Increasing the fin spacing effectively reduces the cold plate's pressure drop, yet its effect on improving the total thermal resistance is not significant. After systematically analyzing all parameters, it was determined that liquid metal exhibits optimal flow heat-transfer performance at a fin height of 5 mm, a fin spacing of 0.6 mm, and a working fluid velocity of 0.1 m/s.

Muhammad et al. [48] investigated the flow and heat transfer of liquid metal in rectangular microchannels under fixed heat flux and temperature constraints. The study revealed that liquid metal exhibits outstanding flow and heat-transfer performance under structural parameters of 6 mm channel height, 0.6 mm channel width, and 0.4 mm wall thickness. Furthermore, it was found that for small-channel heat sinks using GaInSn as the working fluid, the thermal resistance is primarily determined by three key parameters: channel height, channel width, and working fluid inlet velocity. The influence of channel width on thermal resistance is significantly greater than that of channel height, indicating that deep, narrow channels are more effective for heat transfer. When the length and

width of the flow channel remain constant, a specific combination of fin thickness and base thickness for the heat sink enables it to achieve minimal thermal resistance.

An et al. [43] investigated the flow and heat-transfer characteristics of liquid gallium-based alloys in rectangular microchannels under fixed heat flux and inlet temperature conditions. The study found that reducing the microchannel width and increasing the liquid-metal flow rate can enhance the heat-transfer performance of the heat sink.

Mohebbi et al. [49] and Yang et al. [50] primarily investigated the effects of heat sink inlet/outlet dimensions and flow structure configurations on the performance of liquid-metal heat sinks. The results indicate that under different inlet dimensions, the heat-transfer performance of the liquid-metal heat sink remains largely stable, but the pressure drop undergoes significant changes. Moreover, the smaller the inlet dimensions of the heat sink, the greater the pressure drop. Simulation studies also reveal that heat sinks with vertical inlet and outlet configurations exhibit the lowest pressure drop and minimal temperature rise, enabling liquid metal to deliver outstanding heat-transfer performance under these conditions.

Beyond straight microchannels, topology-optimized flow paths have been proposed to improve flow distribution and temperature uniformity. Typical examples include tree-shaped bifurcated channels, T-Y channels, and biomimetic vascular channels. These structures aim to enhance heat transfer by improving flow allocation, increasing mixing, and reducing local thermal non-uniformity. However, the improvement in thermal performance is often accompanied by increased design complexity, manufacturing difficulty, or local pressure loss.

Liu and Li [51] systematically investigated the critical issue of flow distribution within fuel cell flow channels and innovatively designed the tree-like manifold flow channel structure. The tree-shaped converging microchannel adopts a branching and merging flow-path design. By optimizing the length-to-width ratio of the straight section before the branch node, the structure improves flow distribution among different branches, reduces local flow imbalance, and helps achieve a more uniform temperature field. However, its complex topology increases manufacturing difficulty and pressure-loss control requirements. The diverter configuration was developed through multi-parameter optimization analysis based on dual requirements: flow uniformity metrics and pressure drop characteristics. Research findings indicate that the length-to-width ratio (L/W) of the straight pipe section upstream of the flow-directing node is a critical geometric parameter influencing flow distribution downstream of the 90° bend structure. Therefore, appropriately increasing the length of the straight pipe section can significantly enhance flow equilibrium characteristics between branches, thereby effectively promoting the full development of the working fluid flow.

Liu et al. [52] investigated the performance of T-Y channel heat sinks using GaInSn as the coolant. The T-Y microchannel heat exchanger consists of repeated T-Y branching units. The optimized Y-shaped branching angle of approximately 60° can enhance secondary flow and improve temperature uniformity. Compared with conventional straight channels, this structure provides better heat-transfer performance under high-heat-flux conditions, although increased inlet size and flow resistance must be considered. To gain deeper insights into the characteristics of this radiator, researchers employed both numerical simulation and experimental testing methods. They conducted computational analyses of the heat-transfer coefficient and pressure drop of the T-Y channel radiator under six different inlet air velocity conditions. During testing, the peak heat flux density reached 1.6 MW/m^2, and the maximum temperature was controlled within 150 °C. The research findings indicate that the T-Y type channel radiator inherently possesses excellent heat-transfer performance with relatively uniform temperature distribution. Three-dimensional simulations conducted using FLUENT determined that the optimal branching angle for the Y-type channel is 60°. Additionally, it was discovered that adopting an alternating

arrangement for the radiator elements and increasing the heat exchanger inlet volume can effectively enhance the radiator's performance.

Zhang et al. [53] applies "vascular-type" liquid-metal cooling technology in the thermal management of high-power laser diode arrays. The vascular-type liquid-metal heat exchanger mimics biological vascular networks and contains multiple interconnected microchannels. This design increases the heat exchange area and improves heat dissipation capability. GaInSn-based vascular channels have demonstrated effective cooling performance for high-power heat sources, but the complex internal network also introduces challenges in manufacturing precision, flow distribution control, and structural reliability. The author designed a liquid-metal radiator with a distinctive 1.8 mm dimension, featuring a "vascular" configuration with 70 channels. During research on "vascular-type" water cooling and cooling methods using gallium-indium-tin (GaInSn) alloys, the author discovered that thermal resistance due to heat capacity is a key factor affecting cooling efficiency in "vascular-type" liquid-metal cooling processes, whereas this thermal resistance is relatively minor in "vascular-type" water cooling systems. The author conducted flow heat-transfer capability tests and numerical analysis. When using GaInSn for cooling, it effectively dissipated the heat generated by a 2000 W laser diode array, with the maximum temperature on the top surface of the heat sink maintained below 54 °C.

Table 5 summarizes the representative structural parameters of typical liquid-metal cooling channels. It should be noted that the listed parameters are extracted from different studies with different working fluids, heat fluxes, boundary conditions, and evaluation criteria. Therefore, the data in Table 5 are mainly used for qualitative comparison rather than direct quantitative ranking. These studies indicate that the synergistic design of microchannel geometry and liquid-metal coolant is an important route for high-heat-flux cooling. By adjusting channel topology and geometric parameters, liquid-metal flow and heat-transfer performance can be improved, but the accompanying pressure drop and manufacturing constraints must also be considered.

Table 5. Typical structural parameters.

Cooling Structure Type	Key Structural Parameters (Geometric Dimensions)	Flow Characteristics (Inlet Velocity/Reynolds Number)	Heat-Transfer Performance (Nu Number/Temperature Rise)	Pressure Loss/Resistance Characteristics (Pressure Drop/Friction Coefficient)
Tree-shaped bifurcated flow channel	L/W ratio: The key to the longitudinal-to-transverse ratio of the straight pipe section Structure: 90° bend + straight pipe section	Flow uniformity: Significantly affected by L/W Flow state: Fully developed flow	Heat-transfer coefficient: Dependent on the uniformity of flow Trend: Increasing the straight pipe section can enhance the uniformity	Pressure drop: It decreases initially and then stabilizes as the straight pipe section increases Characteristics: The structure is complex and the local resistance is high
T-Y type flow channel	Bifurcation angle: 60° (optimal) Layout: Spaced arrangement	Flow state: There is secondary flow Speed: The air intake speed has a significant impact	Nu number: High Temperature control: Less than 150 °C at 1.6 MW/m^2	Pressure drop: Increases as the inlet volume increases Optimization: Increasing the inlet volume can enhance performance, but it also increases the pump power
Bionic vascular type	Size: 1.8 mm Number of channels: 70 Shape: Tree-like/Vascular-like	Resistance: Key factors such as heat capacity and thermal resistance exist Flow rate: Uneven distribution	Heat dissipation capacity: 2000 W power Temperature: Controlled below 54 °C	Pressure drop: Relatively low (compared to straight pipe) Pressure drop: lower pressure loss
Cylindrical/Circular channel	Diameter: Circular pipe/Tubing Eccentricity: Has an impact	Reynolds number: 20,000–60,000 Buoyancy force: Significantly affects the velocity distribution	Heat-transfer coefficient: Varies with buoyancy force Trend: Enhanced heat transfer under strong buoyancy force	Friction coefficient: Affected by eccentricity and heat flux Range: Fitted within 12–59 MW/m^2 heat flux

3.3.2. Feasibility Analysis

The feasibility analysis in this section is a qualitative engineering comparison based on the literature summarized in Section 3.3.1 and Table 5. It is not derived from new experiments or new numerical simulations conducted in this review. Because the cited studies use different working fluids, heat fluxes, channel dimensions, inlet velocities,

and boundary conditions, the comparison focuses on relative trends rather than absolute performance values. The evaluation criteria include heat-transfer enhancement potential, pressure drop, temperature uniformity, design complexity, manufacturing difficulty, and engineering applicability.

1. Dendritic Bifurcating Flow Channel

Advantages: The dendritic structure can effectively solve the problem of uneven flow distribution. Its "branching-convergence" mechanism can ensure the balanced flow in each branch, thereby achieving uniform temperature distribution on the combustion chamber wall and avoiding local overheating.

Challenges: The aspect ratio (L/W) of the straight pipe section is a key constraining parameter. In engineering manufacturing, it is necessary to process micro-structured dendritic pipes that meet the L/W requirements within the limited wall thickness (usually only a few millimeters). This places extremely high demands on micro-processing technologies (such as micro-milling and lithography).

Conclusion: Tree-shaped bifurcated channels show good potential for improving flow uniformity and temperature uniformity, but their design and manufacturing complexity are relatively high. Their engineering performance is also sensitive to geometric errors and flow maldistribution.

2. T-Y Type Flow Channel

Advantages: The T-Y structure performs best at a 60° bifurcation angle. Compared to the dendritic structure, its geometric shape is more regular and can be easily achieved through existing mechanical processing or additive manufacturing (3D printing). Numerical simulations show that its temperature distribution is uniform, and it can withstand an extremely high heat flux of 1.6 MW/m^2.

Challenges: The "spaced arrangement" and inlet size need to be optimized. In the limited combustion chamber wall space of a hypersonic engine, how to compactly arrange these T-Y units to maximize the heat exchange area is a structural design challenge.

Conclusion: The T-Y structure offers a relatively balanced compromise among heat-transfer performance, pressure drop, and manufacturability. Therefore, it has comparatively high engineering applicability among the reviewed microchannel structures.

3. Bionic Vascular Type

Advantages: This structure mimics biological blood vessels and has extremely high heat dissipation efficiency (with a heat dissipation capacity of 2000 W). Its core advantage lies in low flow resistance, which is crucial for liquid-metal cooling systems as it means lower power consumption for the driving pump and a more compact system.

Challenges: This is the most difficult of the three structures to manufacture. The complex network of 70 pathways requires extremely high molding precision. Additionally, "thermal capacitance and thermal resistance" are key factors, meaning that in transient flight conditions (where the heat load changes rapidly), the thermal response characteristics of this structure require more complex control algorithms.

Conclusion: Biomimetic vascular channels show strong heat-transfer potential, but their engineering maturity remains relatively low. Their application is currently limited by manufacturing complexity, structural reliability, and the need for transient thermal control validation.

Table 6 presents a qualitative engineering evaluation of tree-shaped, T-type, Y-type, and biomimetic vascular channels. The ranking is based on the relative trends reported in the cited literature rather than on a unified experimental database. Therefore, Table 6 should be interpreted as a comparative engineering guide, not as a definitive quantitative ranking. In future work, a standardized evaluation method based on the same working fluid, heat flux, inlet velocity, channel volume, and pressure-drop constraint is still needed.

Table 6. Qualitative engineering comparison of typical microchannel structures based on literature-reported trends.

Metric	Dendritic Bifurcating Flow Channel	T-Type	Y-Type	Bionic Vascular Type
PEC	High	Low	High	Highest
Pressure Drop	Medium	High	Medium–Low	Low
Temperature Uniformity	Very High	Low	High	Extremely High
Design Complexity	High	Low	Medium	Very High
Manufacturing Difficulty	Medium	Low	Medium	High
Engineering Practicality	High	Moderate	Highest	Advanced Applications

Overall, the T-shaped structure is simple to manufacture and has limited overall performance, making it suitable for scenarios with high requirements for cost and process; the Y-shaped structure achieves a good balance between practicality and performance; the tree-like fractal structure has obvious advantages in temperature uniformity and heat exchange performance, but its design and manufacturing costs are high; the biomimetic vascular structure has the best overall heat exchange performance, but it is complex and is more suitable for high-end applications with extremely high heat dissipation requirements.

4. Applications of Liquid-Metal Cooling in Hypersonic Vehicles

This section reviews representative applications of liquid-metal cooling in hypersonic-vehicle thermal protection, with emphasis on combustion-chamber wall cooling and liquid-metal/fuel coupled heat exchange. Different from Section 3, which focuses on general flow and heat-transfer mechanisms, this section discusses how these mechanisms are reflected in engine-relevant cooling channels under one-sided high-heat-flux heating. The available studies mainly include numerical simulations and limited experimental validations; therefore, the following discussion focuses on comparative trends, physical interpretation, and engineering implications rather than universal quantitative conclusions.

To evaluate the potential of liquid metals for combustion-chamber thermal protection, previous studies have compared liquid-metal coolants with conventional hydrocarbon fuels in wall-cooling channels. The main concern is whether liquid metals can reduce wall temperature, alleviate thermal stratification caused by one-sided heating, and transfer the absorbed heat to fuel or power-generation systems for further energy utilization.

Chen [11] compared the heat-transfer performance of GaInSn and n-decane in a hypersonic-engine combustion-chamber cooling channel under the same one-sided heating condition. The main simulation parameters are listed in Table 7.

Table 7. Boundary conditions and input parameters for the GaInSn and n-decane cooling-channel simulations.

Working Fluid	Mass Flow (g/s)	Inlet Temperature (K)	Outlet Pressure (MPa)	One-Sided Heat Flux (MW/m^2)
GaInSn ($Ga_{68.5}In_{21.5}Sn_{10}$)	11.8	330	0.1	1.4
n-Decane (n-Decane)	0.8	330	3	

In the simulation, the coolant enters from the channel inlet and flows along the axial direction. The normalized axial coordinate is defined as x/L, where x is the distance from the inlet and L is the total channel length. One wall of the cooling channel is subjected to a prescribed heat flux to represent combustion-side heating, while the other walls are treated according to the boundary conditions reported in [11]. The channel-height direction is used to evaluate thermal stratification across the cross-section.

Since the combustion chamber cooling passages are heated on one side only, the temperature distribution of the cooling medium along the height of the cooling passages exhibits non-uniformity, resulting in thermal stratification. In hypersonic vehicle combustion chambers, coolants with relatively low mass flow rates subjected to high-heat-flux heating exacerbate thermal stratification phenomena [54]. Figures 1 and 2 present the temperature

distributions of n-decane and GaInSn alloy along the height direction at different axial locations under a one-sided heat flux of 1.4 MW/m^2. As shown in Figure 1, n-decane exhibits obvious temperature gradients at different axial positions, especially in the upstream region, indicating a non-uniform heat absorption process. With the increase of axial distance, the temperature profiles gradually converge, and the temperature distribution becomes more uniform due to the development of flow and heat transfer.

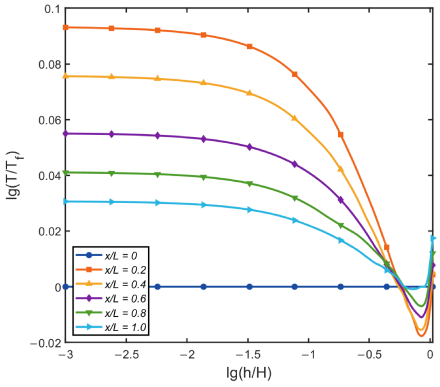

Figure 1. Temperature distribution of n-decane along the height direction at different axial locations [11].

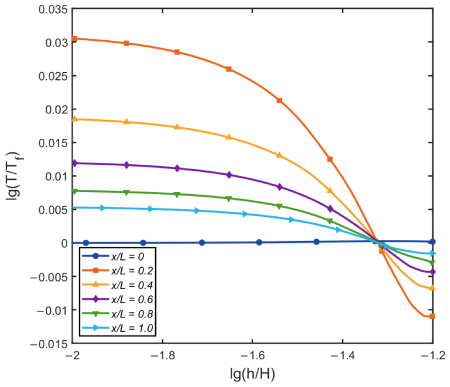

Figure 2. Temperature distribution of GaInSn alloy along the height direction at different axial locations [11].

Compared with n-decane, Figure 2 shows that GaInSn exhibits a more stable temperature distribution with smaller variations among different axial locations. The reduced temperature difference along the height direction indicates improved thermal uniformity and weaker thermal stratification. This behavior is mainly attributed to the higher thermal conductivity of GaInSn, which enhances heat diffusion and improves the cooling performance under high-heat-flux conditions.

Figure 3a shows the distribution curves of the mainstream temperature and the combustion chamber side wall temperature along the flow direction for n-decane and GaInSn in the combustion chamber cooling channel. When using GaInSn for cooling, the temperature rise rates of both the alloy and the cooled combustion chamber side wall gradually converge toward a fixed value. For n-decane, the bulk temperature reaches approximately 800 K near x/L = 0.5, where thermal cracking may occur according to the cited study. Although endothermic cracking can provide an additional chemical heat sink, it also introduces changes in composition and thermophysical properties and may lead to coking risk. Therefore, the apparent cooling benefit associated with cracking should not be interpreted independently of chemical stability and channel blockage concerns. The lower wall temperature obtained with GaInSn should not be attributed only to differences in heat capacity. It is also related to its much higher thermal conductivity, the weak temperature dependence of thermophysical

properties, an absence of thermal cracking, and a more uniform cross-sectional temperature field. From an engineering perspective, GaInSn can serve as an intermediate heat-transfer medium: it absorbs heat from the combustion-chamber wall and then transfers this heat to the fuel through a heat exchanger. In this way, liquid-metal cooling can reduce local wall overheating while still allowing the fuel heat sink to be used downstream.

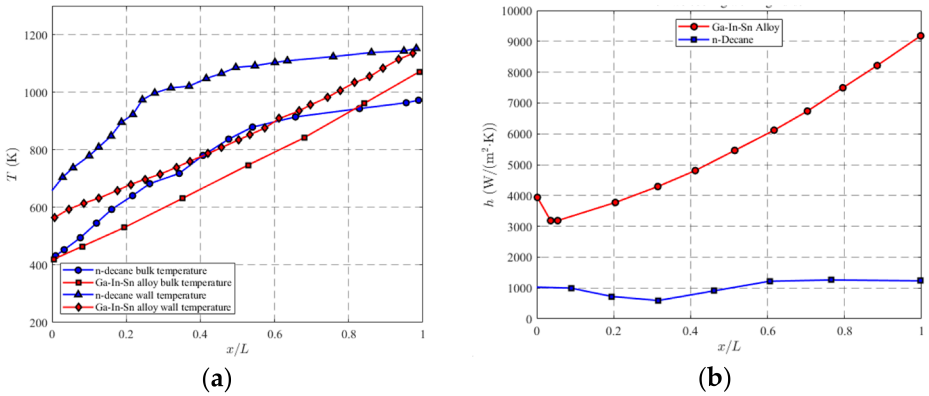

Figure 3. Comparison of cooling effects of n-decane and gallium-indium-tin alloy [11]. (**a**) Temperature distributions of two cooling working fluids, (**b**) Convective heat transfer coefficient distributions of two cooling working fluids.

When a fluid first enters a pipe, the thermal boundary layer is in its development phase at the inlet stage. Consequently, the thermal boundary layer is relatively thin, resulting in a higher convective heat-transfer coefficient. This phenomenon is known as the inlet effect. Figure 3b shows that the GaInSn exhibits a significantly higher heat-transfer coefficient during the inlet stage. As the thermal boundary layer gradually thickens, the heat-transfer coefficient decreases. However, once the fluid flow is fully developed, the heat-transfer coefficient begins to increase again. For n-decane, the heat-transfer coefficient also shows a non-monotonic trend. Near x/L = 0.5, thermal cracking and the accompanying changes in thermophysical properties may affect local heat transfer. However, without direct evidence of turbulence enhancement, this effect should be described as a possible modification of local flow and heat-transfer behavior rather than a confirmed turbulence-induced enhancement. Overall, GaInSn exhibits a higher convective heat-transfer coefficient than n-decane under the simulated conditions, which supports its potential for high-heat-flux wall cooling. Table 8 compares the distribution characteristics of the convective heat-transfer coefficients of gallium-indium-tin alloy and n-decane within the channel.

Table 8. Comparison of convective heat-transfer coefficients.

Position (x/L)	GaInSn Heat-Transfer Coefficient W/(m²·K)	n-Decane Heat-Transfer Coefficient Trend
Inlet section (≈0)	High (entrance effect)	High (entrance effect)
x/L = 0.1	32,000	Gradually decreases
x/L ≈ 0.5	Gradually increases	Thermal cracking induces disturbance, coefficient increases
x/L = 1.0	92,000 (peak value)	Lower than GaInSn
Overall evaluation	Superior, significantly higher heat-transfer performance	Affected by thermal cracking, performance fluctuates

Figures 4 and 5 present the velocity profiles of n-decane and GaInSn at different axial positions, respectively. In these figures, x/Z denotes the normalized streamwise location, and the height coordinate represents the direction normal to the heated wall. After entering the parallel cooling channels of the combustion chamber, the velocity profiles of both fluids develop along the streamwise direction. Due to the boundary layer effect and the no-slip

condition, the fluid velocity near the heated wall is lower than that in the region away from the wall.

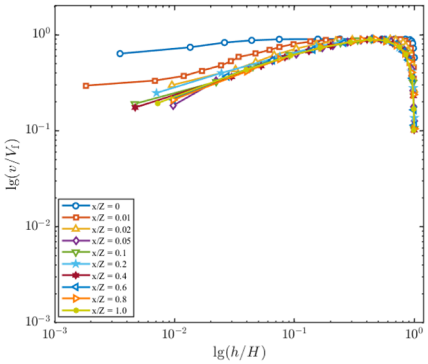

Figure 4. N-decane velocity distribution [11].

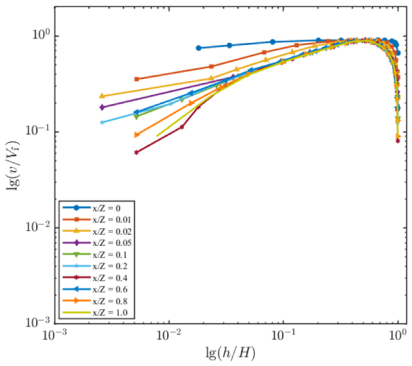

Figure 5. Gallium-indium-tin alloy velocity distribution [11].

For n-decane, the velocity profiles at different x/Z locations show variations during the flow development process. In the upstream region, the velocity distributions differ significantly due to the influence of entrance effects. As the flow proceeds downstream, the velocity profiles gradually become more stable, indicating the continuous development of the flow field inside the cooling channel.

For GaInSn, the velocity profiles also evolve along the axial direction. The velocity near the wall remains relatively low, while the velocity increases with increasing distance from the wall. Compared with the upstream region, the downstream velocity profiles show less variation, suggesting that the influence of the entrance region gradually decreases along the flow direction.

The comparison between n-decane and GaInSn demonstrates that both fluids undergo a similar velocity development process in the parallel cooling channels. The differences in velocity profiles mainly result from the evolution of the flow field along the axial direction. Table 9 compares the velocity distribution characteristics of n-decane and gallium-indium-tin alloy in the channel.

Table 9. Comparison of velocity distribution characteristics.

Comparison Item	n-Decane	GaInSn Alloy
Velocity distribution pattern	Irregular inverted "U-shape" (asymmetric)	Symmetric inverted "U-shape"
Location of maximum velocity	Biased toward combustion-side wall (at x/L = 0.4)	Located at the channel center
Fully developed position	Relatively late	Fully developed at x/L = 0.5
Effect of density variation	Density decreases when heated; significant acceleration near heated wall	Minor variation in thermophysical properties, negligible effect
Flow symmetry	Asymmetric	Symmetric and uniform

Given that aerospace fuel serves as the sole heat sink for hypersonic vehicles, GaInSn must transfer heat absorbed from the combustion chamber walls to the fuel. Therefore, investigating their coupled heat transfer is essential. The authors constructed a liquid metal-aerospace fuel spiral tube heat exchanger for experimental research. When a fluid flows through a helical tube, the curvature of the channel generates a radial pressure gradient and centrifugal effects. These effects may induce Dean-type secondary motion, which is characterized by transverse circulation or a pair of counter-rotating vortices in the tube cross-section. Such motion can enhance radial mixing and disturb the thermal boundary layer, thereby modifying the heat-transfer behavior compared with straight-tube flow [55]. The inner cooling medium within the heat exchanger is GaInSn, which serves as the heat source, while the outer cooling medium is n-decane, acting as the cold source. As shown in Figure 6 the initial simulation conditions include a GaInSn mass flow rate of 9.4 g/s and a n-decane mass flow rate of 1.8 g/s. The simulation results indicate that the velocity distribution of GaInSn within the heat exchanger cross-section remains relatively stable at different cross-sections, with the maximum velocity region located near the spiral tube wall. Meanwhile, the velocity distribution of n-decane varies along the flow passage due to the influence of the channel geometry and flow development. The combined cooling configuration enables the interaction between the two working fluids and provides a coupled flow condition within the heat exchanger.

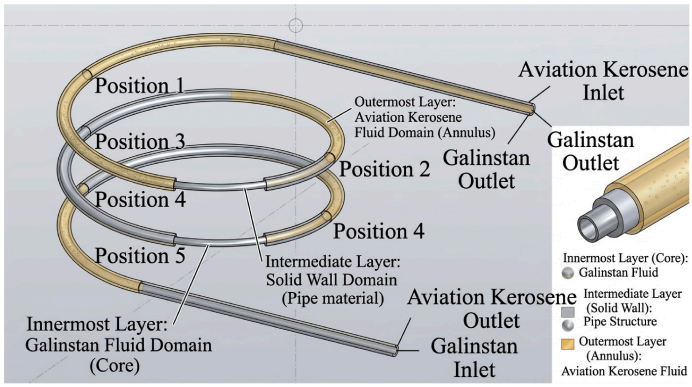

Figure 6. Heat exchanger structure diagram [11].

Table 10 conducts a comprehensive comparison of gallium-indium-tin alloy and n-decane based on multiple performance indicators. The results show that gallium-indium-tin alloy outperforms n-decane in all evaluation indicators. Its temperature distribution is uniform and symmetrical, with a very light degree of thermal stratification (temperature difference less than 1.8%), and the maximum convective heat-transfer coefficient reaches as high as 92,000 W/m^2 at x/L = 1, far exceeding that of n-decane. At the same time, gallium-indium-tin alloy has stable chemical properties and will not undergo thermal cracking, the velocity distribution is symmetrical and an inverted "U" shape, the thermal properties are extremely sensitive to temperature, the wall surface cooling is uniform, and it can still maintain stable operation under extreme thermal conditions. In contrast, the temperature distribution of n-decane is not uniform and asymmetric, the thermal stratification is severe, the heat-transfer coefficient is significantly lower, it is prone to thermal cracking at high temperatures, the velocity field is asymmetric, the density changes significantly with temperature, and the wall surface cooling is uneven. In extreme conditions, its adaptability is relatively weak. In summary, gallium-indium-tin alloy, with its excellent thermal conductivity, chemical stability, and thermal property stability, demonstrates superior comprehensive performance over traditional hydrocarbon fuels in the microchannel cooling field; it is a cooling medium with great application prospects in extreme thermal environments.

Table 10. Comprehensive performance comparison of liquid-metal and conventional hydrocarbon fuel.

Performance Metric	GaInSn Alloy	n-Decane	Advantage
Temperature distribution uniformity	Uniform, symmetric distribution	Non-uniform, asymmetric	GaInSn
Thermal stratification degree	Slight ($\Delta T \leq 1.8\%$)	Severe	GaInSn
Maximum convective heat-transfer coefficient	92,000 W/(m^2·K) (x/L = 1)	Lower than GaInSn; exact maximum value not explicitly reported in Ref. [11]	GaInSn
Chemical stability	Stable, no thermal cracking	Thermal cracking occurs at high temperature	GaInSn
Velocity distribution symmetry	Symmetric inverted "U-shape"	Asymmetric	GaInSn
Thermophysical property stability	Sensitive to temperature	Strongly affected by density variation	GaInSn
Wall-cooling uniformity	Uniform	Non-uniform	GaInSn
Adaptability to extreme thermal conditions	Strong, maintains stable operation	Relatively weak	GaInSn

In summary, existing application-oriented studies indicate that liquid metals are promising intermediate coolants for hypersonic-engine wall thermal protection. Their main advantages include high thermal conductivity, stable thermophysical properties, weak thermal stratification, and the absence of fuel cracking and coking inside the wall-cooling channel. Nevertheless, several engineering issues remain unresolved, including liquid-metal/fuel heat-exchanger design, material compatibility, corrosion control, electromagnetic pumping, system weight, and integration with the fuel supply and power-generation subsystems. Therefore, future application studies should move beyond single-channel performance comparison and focus on integrated liquid-metal/fuel thermal management systems under realistic flight heat-load histories and vibration conditions.

5. Conclusions

This review summarizes the current status of liquid-metal active cooling technology for hypersonic aircraft from three perspectives: flow and heat-transfer characteristics, microchannel structure optimization, and application-oriented thermal protection systems. The reviewed studies indicate that liquid metals provide clear thermal advantages over conventional hydrocarbon fuels, including much higher thermal conductivity, a low Prandtl number, a wide liquid-temperature range, resistance to high-temperature cracking and coking, and compatibility with electromagnetic pumping. These features make liquid metals especially attractive for severe heat loading environments where traditional regenerative cooling is limited by insufficient heat sink capacity and thermal degradation.

From the perspective of flow and heat transfer, the available studies show that channel geometry, inlet velocity, buoyancy, inclination angle, and wall roughness all influence liquid-metal cooling performance. At the structural level, deep and narrow microchannels, tree-shaped channels, T-Y channels, and biomimetic vascular channels can improve heat transfer and temperature uniformity, although these benefits often come with increased pressure drop or manufacturing complexity. At the system level, liquid-metal/fuel dual-channel cooling, waste heat recovery, and thermoelectric conversion schemes demonstrate the potential of liquid metals as intermediate heat-transfer media rather than only as stand-alone coolants.

The reviewed literature also shows that liquid-metal cooling is most meaningful when evaluated as part of an integrated thermal management architecture. Its engineering value lies not only in high heat-transfer capability, but also in its ability to reduce thermal stratification, avoid coking blockage, and enable downstream heat utilization. For this reason, the main contribution of the present review is to compare the reported concepts

in terms of thermal performance, structural feasibility, and application relevance and to clarify where liquid-metal cooling is most suitable in severe heat loading applications.

Author Contributions: Conceptualization, X.H. and H.L.; methodology, Z.D.; software, X.H.; validation, G.S.; investigation, Z.D.; resources, X.H.; data curation, X.H.; writing—original draft preparation, X.H., Z.D. and G.S.; writing—review and editing, X.H. and H.L.; visualization, X.H.; funding acquisition, H.L. and Z.D. All authors have read and agreed to the published version of the manuscript.

Funding: This research was funded by Guangdong Basic and Applied Basic Research Foundation, grant number 2024A1515010637, Guangdong Basic and Applied Basic Research Foundation, grant number 2022A1515110605, and Guangdong Ocean University Undergraduate Innovation Training Program, grant number 202510566035.

Data Availability Statement: No new data were created or analyzed in this study. Data sharing is not applicable to this article.

Acknowledgments: The authors thank the reviewers for their valuable advice on this paper. Furthermore, gratitude and best wishes are offered to the staff and editors at *Aerospace* for their support of this work.

Conflicts of Interest: The authors declare no conflicts of interest.

References

1. Kulkarni, A.; Yadav, S.K.; Kumar, A.; Ram, S. Recent advancements in scramjet engine: A review. *AIP Conf. Proc.* **2023**, *2981*, 090019. [CrossRef]
2. Lv, Z.; Xu, J.; Ge, L.J. Review on the aerodynamic issues of the exhaust system for scramjet and turbine based combined cycle engine. *Prog. Aerosp. Sci.* **2023**, *143*, 100956. [CrossRef]
3. Liu, C.; Ai, J.; Zhang, J.; Li, X.; Zhao, Z.; Huang, W. Research progress of the flow and combustion organization for high-Mach-number scramjet: From Mach 8 to 12. *Prog. Aerosp. Sci.* **2025**, *155*, 100956. [CrossRef]
4. Liu, X.Y.; Wang, M.F.; Liu, J.W.; Ren, X.; Zhang, X. Review and prospect of scramjet engine research. *Acta Aeronaut. Astronaut. Sin.* **2024**, *45*, 218–244.
5. Dang, C.; Cheng, K.; Fan, J.; Wang, Y.; Qin, J.; Liu, G. Performance analysis of fuel vapor turbine and closed-Brayton-cycle combined power generation system for hypersonic vehicles. *Energy* **2023**, *266*, 126426. [CrossRef]
6. Wang, C.; Yu, X.; Ha, C.; Liu, Z.; Fang, J.; Qin, J.; Shao, J.; Huang, H. Thermodynamic analysis for a novel chemical precooling turbojet engine based on a multi-stage precooling-compression cycle. *Energy* **2023**, *262*, 125352. [CrossRef]
7. Dang, C.; Cheng, K.; Xu, J.; Fan, J.; Qin, J.; Liu, G. Performance analysis of a thermal management system based on hydrocarbon-fuel regenerative cooling technology for scramjets. *Energy* **2023**, *285*, 128720. [CrossRef]
8. Wang, Z.; Feng, Y.; Chen, F.; Qin, J. Thermal behavior of steam reforming reaction at different aspect ratios in the scramjet engine cooling channel. *Energy* **2025**, *314*, 134166. [CrossRef]
9. Liu, X.; Wei, L.; Yu, C.; Liu, Z.; Yu, H.; Cao, X. A review of cooling technologies for scramjet engines and the mechanisms of fuel heat absorption and coking in cooling channels. *Fuel* **2026**, *419*, 138733. [CrossRef]
10. Xu, J.; Cheng, K.; Qin, J.; Wang, C.; Liu, Z.; Liu, X. Structure effect on thermal-hydraulic performance in liquid metal—Aviation kerosene printed circuit heat exchanger. *Appl. Therm. Eng.* **2023**, *220*, 119741. [CrossRef]
11. Cheng, K.; Xu, J.; Dang, C.; Qin, J.; Jing, W. Performance evaluation of fuel indirect cooling based thermal management system using liquid metal for hydrocarbon-fueled scramjet. *SSRN Electron. J.* **2022**, *260*, 125068. [CrossRef]
12. Sippel, M.; Wilken, J. Selection of propulsion characteristics for systematic assessment of future European RLV-options. *CEAS Space J.* **2025**, *17*, 89–111. [CrossRef]
13. Cheng, K.L. Performance Study of Combined Power Generation System for Hypersonic Vehicles Based on Cascade Utilization of Cold Sources. Ph.D. Thesis, Harbin Institute of Technology, Harbin, China, 2020.
14. Xu, J.; Yu, H.; Dang, C.; Cheng, K.; Liu, Z.; Qin, J.; Liu, X. Comparison of heat transfer performance between liquid metal and aviation kerosene in the wall cooling channel of aero-engine. *Int. J. Heat Mass Transf.* **2024**, *222*, 125159. [CrossRef]
15. Su, D.-D.; Li, X.-B.; Zhang, H.-N.; Li, F.-C. Molecular dynamics study on boiling characteristics of liquid sodium under different wall temperature: Incipient boiling superheat, heat transfer performance and mechanism. *Appl. Therm. Eng.* **2025**, *264*, 125475. [CrossRef]
16. Yao, Y.; Zhou, T.; Huang, D.; Mao, S.; Zhang, H. Thermophysical properties of liquid gallium: A review. *Ann. Nucl. Energy* **2026**, *234*, 112322. [CrossRef]

17. Wang, T.; An, K.; Sun, P. Liquid metal microchannel cooling for aerospace thermal management. In *Aerospace Frontiers Conference*; Springer Nature: Singapore, 2025; pp. 67–80.
18. Xu, J.; Cheng, K.; Dang, C.; Wang, Y.; Liu, Z.; Qin, J.; Liu, X. Performance comparison of liquid metal cooling system and regenerative cooling system in supersonic combustion ramjet engines. *Energy* **2023**, *275*, 127488. [CrossRef]
19. Cheng, K.; Qin, J.; Jiang, Y.; Lv, C.; Zhang, S.; Bao, W. Performance assessment of multi-stage thermoelectric generators on hypersonic vehicles at a large temperature difference. *Appl. Therm. Eng.* **2018**, *130*, 1598–1609. [CrossRef]
20. Xu, J.; Dang, C.L.; Wang, Y.L.; Wang, S.; Cheng, K.; Qin, J.; Liu, X. Research on heat transfer performance of liquid metal-hydrocarbon fuel double-layer cooling channels for aero-engine walls. *Aeronaut. Sci. Technol.* **2024**, *35*, 16–27.
21. Feng, X.; Zhou, T.; Zang, J.; Zhang, B.; Chen, J. Study on natural circulation heat transfer characteristics of different liquid metals based on factor analysis. *Front. Energy Res.* **2020**, *8*, 123. [CrossRef]
22. Lv, Y.J. Large Eddy Simulation of Turbulent Heat Transfer Characteristics of Liquid Metal in Annular Tubes. Master's Thesis, University of Science and Technology of China, Hefei, China, 2015.
23. Martinelli, R.C. Heat transfer to molten metals. *Trans. ASME* **1947**, *69*, 947–959. [CrossRef]
24. Lyon, R.N. Liquid metal heat transfer coefficients. *Chem. Eng. Prog.* **1951**, *47*, 75–79.
25. Dwyer, O.E. Eddy transport in liquid metal heat transfer. *AIChE J.* **1963**, *9*, 261–268. [CrossRef]
26. Maresca, M.; Dwyer, O.E. Heat transfer to mercury flowing in-line through a bundle of circular rods. *J. Heat Transf.* **1964**, *86*, 180–186. [CrossRef]
27. Werner, R.C.; King, E.C.; Tidball, R.A. Heat transfer with sodium-potassium liquid alloys. *Mech. Eng.* **1949**, *71*, 990–993.
28. Shi, S.K. Experimental study on heat transfer of liquid metal sodium in circular tubes and sleeve tubes. *J. Eng. Thermophys.* **1981**, *2*, 173–180.
29. Wang, C.; Wang, C.L.; Zhang, Y.; Zhang, D.; Tian, W.; Qiu, S.; Su, G. Study on flow and heat transfer characteristics of liquid lead-bismuth alloy in tubes. *At. Energy Sci. Technol.* **2021**, *55*, 822–828.
30. Saxena, A.; Falcone, M.; He, S. LES of the upper plenum of the liquid metal fast reactor under forced flow conditions. *Nucl. Eng. Des.* **2024**, *424*, 113298. [CrossRef]
31. Hong, R.; Yuan, B.Q.; Du, W.J. Heat transfer deterioration mechanism of supercritical CO2 in vertical tube. *CIESC J.* **2023**, *74*, 3309–3319.
32. Yuan, B.; Sun, J.; Xiao, Y.; Ding, G.; Gu, H. Convective heat transfer at low flow in lead-bismuth eutectic. *Nucl. Power Eng.* **2025**, *46*, 128–135.
33. Dzodzo, M.B. Mixed convection heat transfer to liquid metals in vertical channels. *Nucl. Eng. Des.* **2024**, *428*, 113479. [CrossRef]
34. Guo, Y.F.; Su, X.K.; Wang, G.; Chen, Q.J.; Gu, L. Numerical Investigation of Turbulent Mixed Convection of Liquid Metal in Inclined Tube Based on Second-order Differential Heat Flux Model. *At. Energy Sci. Technol.* **2025**, *59*, 360–371.
35. Guo, Y.F.; Su, X.K.; Wang, G.; Lin, H.; Lin, C.; Gu, L. Investigation and development of a second-order differential heat flux model: Mixed convection in inclined pipe with liquid metals. *Nucl. Eng. Des.* **2026**, *430*, 113802. [CrossRef]
36. Vasil'ev, A.Y.; Kolesnichenko, I.V.; Mamykin, A.D.; Frick, P.G.; Khalilov, R.I.; Rogozhkin, S.A.; Pakholkov, V.V. Turbulent heat transfer in inclined tube with sodium. *High Temp.* **2015**, *60*, 1305–1309. [CrossRef]
37. Wu, T.; Wang, L.; Tang, Y.; Yin, C.; Li, X. Flow and Heat Transfer Performances of Liquid Metal Based Microchannel Heat Sinks under High Temperature Conditions. *Micromachines* **2022**, *13*, 95. [CrossRef] [PubMed]
38. Xi, W.Y.; Wang, Y.W.; Huai, X.L. Forced convection heat transfer of lead-bismuth eutectic. *J. Eng. Thermophys.* **2016**, *37*, 586–591.
39. Fico, F.; Langella, I.; Xia, H. LES of magnetohydrodynamics and heat transfer in liquid metal flow. *Phys. Fluids* **2023**, *35*, 055106. [CrossRef]
40. Kadivar, M.; Garg, H. Turbulent heat transfer over roughness: Review. *Int. J. Thermofluids* **2025**, *26*, 100967. [CrossRef]
41. Zhang, X.; Feng, W.; Yang, X.; Yu, H.; Deng, J.; Du, S. Investigation into the flow and heat transfer characteristics in liquid metal cooled narrow rectangular channel with rough surfaces. *Case Stud. Therm. Eng.* **2025**, *72*, 106404. [CrossRef]
42. Huang, S.Z.; Zhu, Q.H.; Gao, X.W. Heat transfer in corrugated tubes. *J. Propuls. Technol.* **2019**, *40*, 95–106.
43. An, K.; Su, Z.; Zhang, M.; Deng, Y. Liquid metal-based micro/mini-channel heat transfer: Progress, challenges, and opportunities. *Appl. Therm. Eng.* **2024**, *250*, 123551. [CrossRef]
44. Chen, W.; Yu, S.; Yao, Y.; An, Z.; Bi, A.; Zhang, W.; Wang, S.; Wang, Y. Liquid metal-based chip cooling technologies: A review. *J. Therm. Sci.* **2025**, *34*, 2009–2045. [CrossRef]
45. Chen, Y.S.; Ruan, D.; Liu, Y.B.; Zheng, T.; Zhang, S.; Ma, X. Topology optimization and performance research of microchannel heat exchangers. *CIESC J.* **2024**, *75*, 823–835.
46. Zhao, H.; Ma, H.; Yan, X.; Yu, H.; Xiao, Y.; Xiao, X.; Liu, H. Hydrothermal performance in micro-channel heat sink. *Micromachines* **2023**, *14*, 1818. [CrossRef] [PubMed]
47. Zhao, L. Thermal control of microchannel cooling plates. *Environ. Technol.* **2021**, *39*, 134–144.
48. Muhammad, A.; Selvakumar, D.; Wu, J. Laminar flow in liquid metal mini-channel heat sink. *Int. J. Heat Mass Transf.* **2020**, *150*, 119265. [CrossRef]
49. Mohebbi, R.; Zarei, M.; Hasani, M. Cooling performance of mini-channel heat sink. *Int. J. Thermofluids* **2024**, *22*, 100627. [CrossRef]

50. Yang, X.H.; Tan, S.C.; Liu, J. Flow and heat transfer in small channel heat sinks. *J. Eng. Thermophys.* **2019**, *40*, 916–925.
51. Liu, H.; Li, P. Flow distribution in bifurcation channels. *Int. J. Heat Fluid Flow* **2013**, *40*, 164–179. [CrossRef]
52. Liu, H.L.; An, X.K.; Wang, C.S. Heat transfer of T-Y microchannel heat sink. *Int. J. Therm. Sci.* **2017**, *120*, 202–219. [CrossRef]
53. Zhang, X.-D.; Li, X.-P.; Zhou, Y.-X.; Yang, J.; Liu, J. Vascularized liquid metal cooling. *Appl. Therm. Eng.* **2019**, *162*, 114212. [CrossRef]
54. Xie, P.Y.; Zhang, X.B. Thermal stratification in supercritical hydrogen. *Numer. Heat Transf. A* **2020**, *77*, 913–929. [CrossRef]
55. Liu, Y.L.; Fu, Y.C.; Wen, J.; Qi, S. Spiral tube heat exchanger design. *J. Propuls. Technol.* **2021**, *42*, 1087–1093.

Disclaimer/Publisher's Note: The statements, opinions and data contained in all publications are solely those of the individual author(s) and contributor(s) and not of MDPI and/or the editor(s). MDPI and/or the editor(s) disclaim responsibility for any injury to people or property resulting from any ideas, methods, instructions or products referred to in the content.